Article

Immunity

Enteric Viruses Ameliorate Gut Inflammation via Toll-like Receptor 3 and Toll-like Receptor 7-Mediated Interferon-β Production

Graphical Abstract

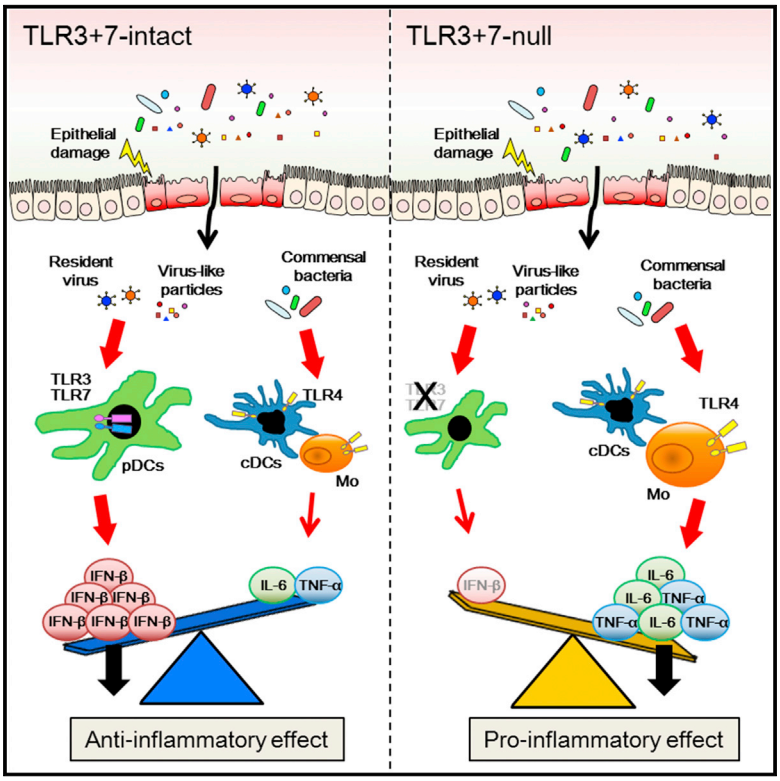

Authors

Jin-Young Yang, Min-Soo Kim, Eugene Kim, ..., Hyun-Jeong Ko, Jin-Woo Bae, Mi-Na Kweon

Correspondence

baejw@khu.ac.kr (J.-W.B.), mnkweon@amc.seoul.kr (M.-N.K.)

In Brief

The role of gut resident viruses in the maintenance of homeostasis is unclear. Kweon and colleagues show the sensing of gut viruses by TLR3 or TLR7 enhances the production of interferon-β that dampens inflammation.

Highlights

- Pre-treatment with an antiviral cocktail results in severe colitis
- Treatment with TLR3+7 agonists and inactivated rotavirus ameliorates colitis
- *Tlr3*$^{-/-}$*Tlr7*$^{-/-}$ mice are more susceptible to colitis
- TLR3+7 agonists stimulate IFN-β secretion by pDCs from inflamed colon

Accession Numbers

GSE79241

Yang et al., 2016, Immunity *44*, 889–900
April 19, 2016 ©2016 Elsevier Inc.
http://dx.doi.org/10.1016/j.immuni.2016.03.009

CellPress

Immunity
Article

Enteric Viruses Ameliorate Gut Inflammation via Toll-like Receptor 3 and Toll-like Receptor 7-Mediated Interferon-β Production

Jin-Young Yang,[1,9] Min-Soo Kim,[2,9] Eugene Kim,[1,9] Jae Hee Cheon,[3,9] Yong-Soo Lee,[1] Yeji Kim,[1] Su-Hyun Lee,[1] Sang-Uk Seo,[4] Seung-Ho Shin,[5] Sun Shim Choi,[5] Bumseok Kim,[6] Sun-Young Chang,[7] Hyun-Jeong Ko,[8] Jin-Woo Bae,[2,*] and Mi-Na Kweon[1,*]

[1]Mucosal Immunology Laboratory, Department of Convergence Medicine, University of Ulsan College of Medicine/Asan Medical Center, Seoul 05505, Korea
[2]Department of Life and Nanopharmaceutical Sciences and Department of Biology, Kyung Hee University, Seoul 02447, Korea
[3]Department of Internal Medicine and Institute of Gastroenterology, Yonsei University College of Medicine, Seoul 03722l, Korea
[4]Department of Medicine, Wide River Institute of Immunology, Seoul National University College of Medicine, Seoul 03080, Korea
[5]Department of Medical Biotechnology, College of Biomedical Science, Kangwon National University, Chuncheon 24341, Korea
[6]Laboratory of Pathology (BK21 Plus Program), College of Veterinary Medicine, Chonbuk National University, Iksan 54596, Korea
[7]Laboratory of Microbiology, College of Pharmacy, Ajou University, Suwon 16499, Korea
[8]Laboratory of Microbiology and Immunology, College of Pharmacy, Kangwon National University, Chuncheon 24341, Korea
[9]Co-first author
*Correspondence: baejw@khu.ac.kr (J.-W.B.), mnkweon@amc.seoul.kr (M.-N.K.)
http://dx.doi.org/10.1016/j.immuni.2016.03.009

SUMMARY

Metagenomic studies show that diverse resident viruses inhabit the healthy gut; however, little is known about the role of these viruses in the maintenance of gut homeostasis. We found that mice treated with antiviral cocktail displayed more severe dextran sulfate sodium (DSS)-induced colitis compared with untreated mice. DSS-induced colitis was associated with altered enteric viral abundance and composition. When wild-type mice were reconstituted with Toll-like receptor 3 (TLR3) or TLR7 agonists or inactivated rotavirus, colitis symptoms were significantly ameliorated. Mice deficient in both TLR3 and TLR7 were more susceptible to DSS-induced experimental colitis. In humans, combined TLR3 and TLR7 genetic variations significantly influenced the severity of ulcerative colitis. Plasmacytoid dendritic cells isolated from inflamed mouse colon produced interferon-β in a TLR3 and TLR7-dependent manner. These results imply that recognition of resident viruses by TLR3 and TLR7 is required for protective immunity during gut inflammation.

INTRODUCTION

Dynamic interactions between gut microbiota and the host immune system are important for gut homeostasis because the host is continuously exposed to trillions of indigenous microorganisms, which are composed of bacteria, archaea, fungi, and viruses (Hooper et al., 2012; Virgin, 2014). Metagenomic studies show that the microbiome of healthy humans and animals includes many viral genes (e.g., DNA and RNA) and that the intestines and skin of healthy humans are associated with viruses that replicate in eukaryotic cells (i.e., eukaryotic viruses) and prokaryotic cells (i.e., bacteriophages) (Phan et al., 2011; Reyes et al., 2010). Commensal bacteria are critically involved in various physiological functions in the gut, and microbial imbalance (i.e., dysbiosis) might cause intestinal pathology such as inflammatory bowel diseases (IBD) (Xavier and Podolsky, 2007); however, little is known about the role of resident viruses in controlling intestinal homeostasis and how these viruses interact with the host immune system.

Metagenomic studies of resident viruses in the healthy gut found that temperate bacteriophages are the predominant viral group. They are assembled and propagated stably within the bacterial host chromosome (Minot et al., 2013; Reyes et al., 2010). A number of different types of eukaryotic viruses (e.g., herpesviruses, poxviruses, picovirnaviruses, and plant-infecting viruses) have also been detected in the healthy gut virome, although they are less abundant and largely derived from diet (Kim et al., 2011; Zhang et al., 2006). Exogenous pathogenic eukaryotic viruses are more predominantly detected in the ill with various gastrointestinal diseases than in healthy individuals (Finkbeiner et al., 2008; Victoria et al., 2009). Pathogenic viruses such as human noroviruses directly induce acute gut inflammation (Basic et al., 2014), and increase the incidence of Crohn's disease (CD) (Cadwell et al., 2010). Conversely, murine noroviruses (MNV) stimulate the proliferation of gut epithelial and immune cell populations such as the commensal bacteria, thereby promoting the development and function of the mucosal immune system (Kernbauer et al., 2014); however, much less is known about the contribution of resident viruses in healthy gut including the possibility that they might elicit innate immune responses.

Crosstalk between resident viruses and the innate immune system is initiated by pattern-recognition receptors (PRRs) that detect viral components, such as genomic DNA, single- and double-stranded RNA (ssRNA and dsRNA, respectively), and RNA with 5′-triphosphate ends and viral proteins (Takeuchi

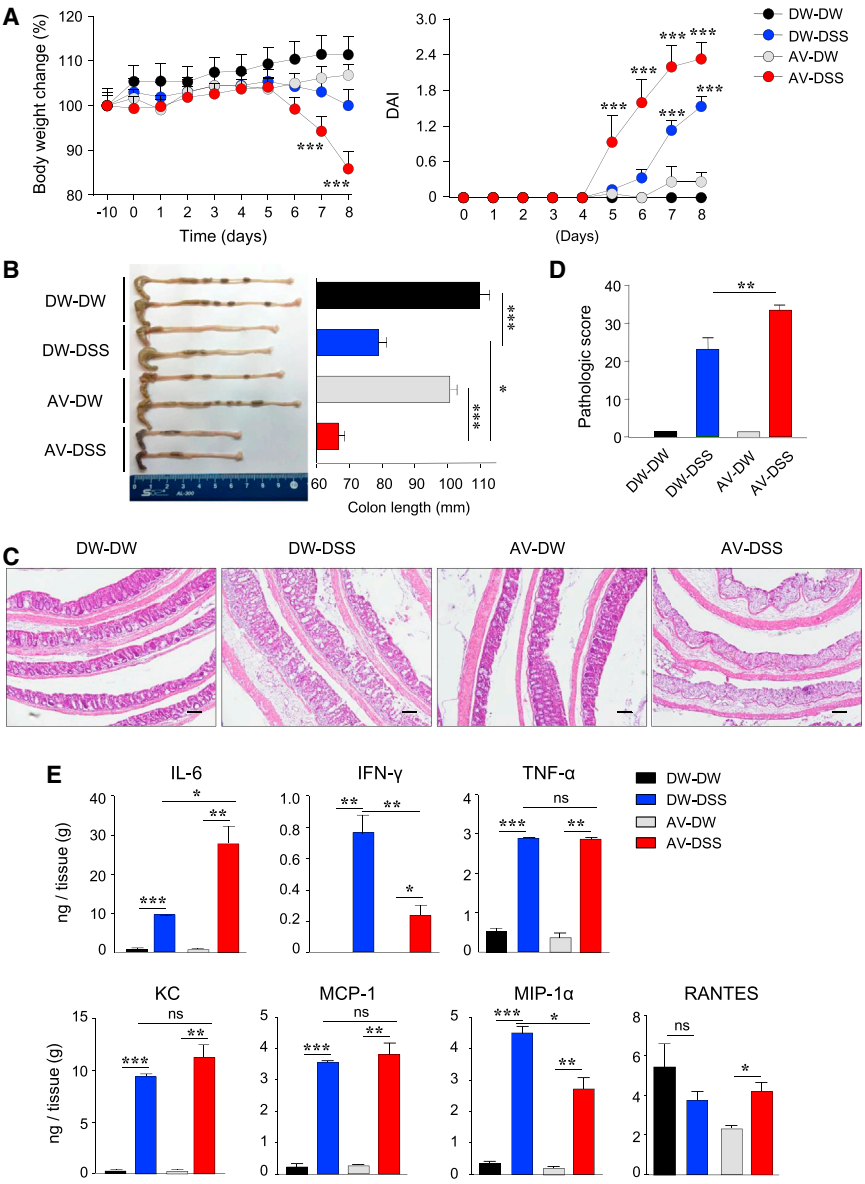

Figure 1. Dextran Sulfate Sodium-Induced Colitis Is Exacerbated with Decreased Virus Load

Mice were perorally administered anti-viral cocktail (AV; ribavirin, lamivudine, acyclovir) for 10 days before DSS treatment.

(A) Body weight change (left panel) was monitored and disease activity index (right panel) was scored for 8 days following 2.5% DSS treatment as described in Experimental Procedures.

(B) Colon length was measured 8 days after DSS treatment.

(C and D) Histologic changes by H&E staining were analyzed based on a cumulative scoring system (range, 0–40). Scale bar represents 100 μm.

(E) Cytokine (IL-6, IFN-γ, and TNF-α) and chemokine (KC, MCP-1, MIP-1α, and RANTES) levels were measured in colon homogenate by ProcartaPlex Multiplex Immunoassays. All data are mean ± SEM of ≥ 2 independent experiments. Statistical analyses were done with two-tailed t test with Mann-Whitney test. *$p < 0.05$, **$p < 0.01$, ***$p < 0.001$; ns, not significant. DW, distilled water.

munity-wide scale. Our results suggest that TLR3 or TLR7 ligation with resident viruses plays a crucial role in intestinal homeostasis by way of protective interferon-β (IFN-β) secreted mainly by plasmacytoid dendritic cells (pDCs).

RESULTS

Resident Enteric Viruses Protect Mice from Dextran Sulfate Sodium-Induced Colitis

To address the role of enteric virus in the pathogenesis of intestinal inflammation, we first treated BALB/c wild-type (WT) mice with antiviral (AV) cocktail (ribavirin, lamivudine, and acyclovir) for 10 days before dextran sulfate sodium (DSS) treatment (2.5% w/v). We hypothesized that decreased viral load in the intestine would have a beneficial effect on intestinal inflammation; however, we found that mice treated with the AV cocktail (AV-DSS) had more severe colitis than AV-untreated mice administered DSS in distilled water (DW-DSS). The AV-treated mice showed more severe clinical symptoms, including body weight loss, stool consistency, and gross bleeding as shown by disease activity index (DAI) than AV-untreated mice (Figure 1A). Severe colitis was also confirmed by shortened colons in AV-treated mice (Figure 1B). Histologic analysis of colons from AV-treated mice showed complete destruction of epithelial integrity, loss of crypts, submucosal edema, and intense infiltration of inflammatory cells (Figure 1C). The histological severity of AV-treated mice was quantified by pathologic scoring (Figure 1D). To further assess pathologic changes in protein levels, we analyzed the secreted amounts of cytokines and chemokines in colon tissue homogenates. Amounts of inflammatory

and Akira, 2010). Toll-like receptors (TLRs) are important PRRs for detecting both dsRNA and ssRNA, which are recognized by TLR3 and TLR7, respectively. TLRs serve as sentinels against pathogens and initiate inflammatory and immune defense responses. It is not clear how to distinguish between pathogenic and commensal microbes because microbial products recognized by TLRs are not specific to pathogens as they are also produced by commensal microbes. One study showed that commensal bacteria-depleted mice recovered from aberrant intestinal inflammation after administration of lipoteichoic acid, a TLR2 agonist or lipopolysaccharide (LPS), a TLR4 agonist (Rakoff-Nahoum et al., 2004). We wondered whether a protective effect of TLRs in intestinal inflammation is confined to recognition of commensal bacteria or whether other microbes, such as viruses, might also be involved.

In the present study, we observed an unexpected protective role of resident viruses recognized by TLR3 and TLR7 on a com-

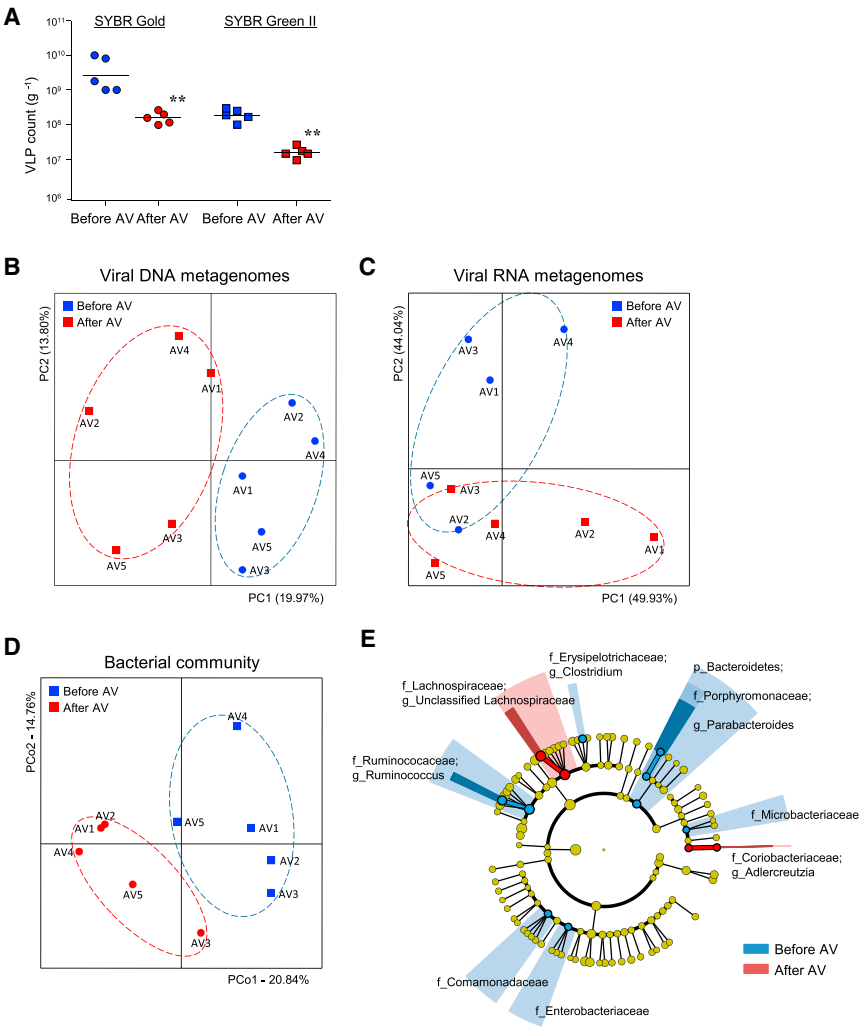

Figure 2. AV Cocktail Influences Abundance and Composition of Gut Viral and Bacterial Communities

(A) Numbers of fecal virus-like particles (VLPs) stained with SYBR Gold for DNA viruses and SYBR Green II for RNA viruses before and after AV cocktail treatment (one-tail Mann-Whitney *U* test, $^{**}p < 0.01$). Communities of enteric viruses of BALB/c WT mice before and after AV cocktail treatment were compared using fecal VLP-derived (B) DNA metagenomes ($p < 0.05$, PERMANOVA on Jaccard distance) and (C) RNA metagenomes ($p < 0.05$, PERMANOVA on Hellinger distance).

(D) Bacterial communities before and after AV treatment were compared using 16S rRNA gene-based community analysis ($p < 0.05$, PERMANOVA on unweighted UniFrac distance).

(E) Composition differences at genus level were determined by linear discriminant analysis using LEfSe.

cytokines (i.e., IL-6) and chemokines (i.e., KC and MCP-1) were higher in the colon tissues of AV-treated mice than in those of WT mice with DSS-induced colitis (Figure 1E). Among the AV agents, acyclovir was most effective for evaluation of enteric virus protection against DSS-induced colitis (Figure S1). Treatment with AV cocktail alone resulted in no significant changes in body weight, DAI, colon length, patho-physiological changes, and cytokines or chemokines (Figure 1). These results suggest that commensal viruses play an indispensable role for protection against DSS-induced colitis.

AV Cocktail Alters the Abundance and Composition of Gut Viral and Bacterial Communities

To examine the effect of an AV cocktail on the abundance of enteric viruses, we isolated virus-like particles (VLPs) from the feces of naive BALB/c mice before and after AV cocktail treatment. Fecal VLPs were stained with SYBR Gold for DNA viruses and Green II for RNA viruses (Figure S2A). At steady-state, we found a mean of 9.54 log ± 0.39 VLPs g^{-1} for DNA viruses and 8.19 log ± 0.17 VLPs g^{-1} for RNA viruses in the feces of naive BALB/c mice (Figure 2A). After AV cocktail treatment, fecal VLPs declined to a mean of 8.27 log ± 0.18 VLPs g^{-1} for DNA viruses (3.44 ± 1.37% before treatment) and averaged 7.18 log ± 0.16 VLPs g^{-1} for RNA viruses (8.16 ± 3.13% before treatment) in naive BALB/c mice (Figure 2A), indicating that AV cocktail significantly decreased the abundance of enteric DNA and RNA viruses.

To identify the genotypic changes of enteric DNA and RNA viruses, we conducted a metagenomic analysis of fecal VLP-derived metagenomic DNA and RNA using Illumina MiSeq sequencing. After quality filtering and removal of host-derived sequences, we obtained a mean of 728,265 ± 142,750 and 559,058 ± 158,391 paired-end sequences per sample in DNA and RNA metagenomes, respectively (Table S1). The sequences were contig-assembled, clustered, and size-based normalized. We generated a mean of 1,225 ± 533 contigs per sample in DNA metagenomes and 284 ± 69 in RNA metagenomes (Table S1). Using contig-based sequence profiles, we compared the genotypes of enteric DNA and RNA viral communities according to AV cocktail treatment. In Jaccard and Hellinger distance-based principal coordinate analysis (PCoA), before and after paired samples of the VLP-derived metagenomes were distant from each other, and fecal VLP-derived DNA (Figure 2B) and RNA (Figure 2C) metagenomes were clustered by AV cocktail treatment ($p < 0.05$, PERMANOVA). To identify which enteric viruses are primarily affected by AV cocktail treatment, we identified the contigs of fecal VLP-derived metagenomes using BLAST searches against NCBI non-redundant protein database and NCBI Refseq viral genomes (*E*-value < 10^{-5}). In both DNA and RNA metagenomes, we could only identify fewer than 30% of total contigs, indicating that the majority of enteric viruses were not characterized as previously described (Kim et al., 2011; Reyes et al., 2010). The identified contigs were bacteria, bacteriophages, mobile genetic elements, and viruses (Figures S2B and S2C). The contigs assigned to bacteria were

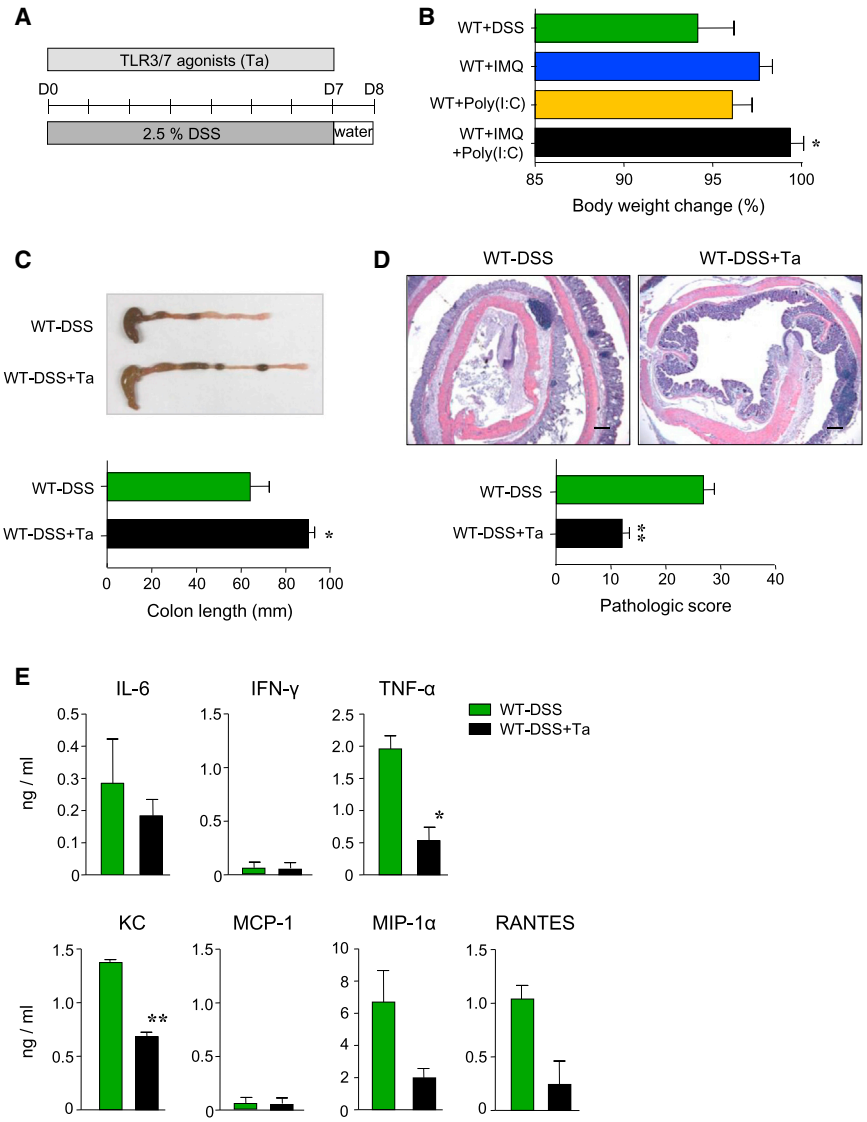

Figure 3. Treatment with Toll-like Receptor (TLR) 3+7 Agonists Attenuate DSS-Induced Colitis

BALB/c wild-type (WT) mice were treated with agonists for TLR3 (Poly I:C) or TLR7 (Imiquimod; IMQ) or both (Poly I:C+IMQ) during DSS feeding. Treatment time lines for TLR3+7 agonists (Ta) (A) and body weight changes (B).

(C) Colon length 8 days after DSS treatment.

(D) Histologic changes were detected and scored in a blinded manner. Results shown are representative of three independent experiments, each with $\geq$ 6 mice per group. Scale bar represents 100 μm.

(E) Cytokine and chemokine levels were measured in culture supernatants by cytokine bead array assay. CD11b$^+$ cells were isolated from colon tissues of DSS-treated WT mice and stimulated with Ta in vitro for 3 days. *p < 0.05, **p < 0.01 versus WT-DSS group.

phage-like sequences integrated in bacterial genomes, and the contigs assigned to bacteriophages, mobile genetic elements, or viruses were associated with uncultured environmental samples or with single-stranded DNA viruses. Interestingly, we found an increase in the richness and abundance of *Caudovirales* bacteriophages in the enteric DNA virome of the mice treated with an AV cocktail (Figures S3A–S3C), which corresponds with findings in a cohort of IBD patients (Norman et al., 2015). These results indicate that the genotypic changes in the community composition of enteric DNA and RNA viruses are implicated in deterioration against DSS-induced colitis by AV cocktail treatment.

Because of the unexpected effect of the AV cocktail on gut microbiota, we conducted gut bacterial community analysis based on the V1-V2 regions of 16S rRNA gene sequences using 454-pyrosequencing. In UniFrac-based PCoA analysis, the samples were clustered separately dependent on AV cocktail treatment ($p < 0.05$, PERMANOVA) (Figure 2D). By LEfSe analysis, we determined the bacterial groups were most changed by AV cocktail treatment. The genus *Ruminococcus* was largely depleted and the unclassified *Lachnospiraceae* was highly enriched after treatment (Figure 2E). However, bacterial diversity and richness were not affected by AV cocktail treatment (Figures S3D and S3E). Although the underlying mechanisms are not known, the antiviral agents also influence few specific bacterial taxa of the gut microbiota.

Activation of TLR Signals Targeting Viral Recognition Ameliorates Intestinal Inflammation

Because enteric viruses might interact with the innate immune system by engaging with TLRs (e.g., TLR3 and TLR7), we next investigated the involvement of innate immunity on the protective effect of resident viruses on intestinal inflammation. To address this hypothesis, we administered WT mice agonists for TLR3 (Poly I:C) and TLR7 (Imiquimod, IMQ) and treated them with DSS (Figure 3A). Despite identical intake of DSS water (data not shown), the TLR3 and TLR7 agonists (Ta) were significantly protective for weight loss and colitis symptoms, whereas mice treated with a single agonist were not protected (Figure 3B). Attenuated inflammation in the colons of Ta-treated mice was supported by longer colon length and milder pathology than found in the non-treated group (Figures 3C and 3D). To evaluate the protective function of Ta on innate immune cells, we isolated CD11b$^+$ cells from colon tissues of DSS-treated WT mice and stimulated with Ta in vitro for measurement of cytokine and chemokine levels. The fact that amounts of cytokines (e.g., TNF-α) and chemokines (e.g., KC) in the culture supernatant were significantly reduced by Ta stimulation (Figure 3E), indicates the protective role of enteric viruses resulted from regulation of inflammatory signals in innate immune cells. These findings suggest that the protective effect of enteric viruses might be derived from ligation of TLRs.

In order to further confirm the protective role of resident enteric viruses, we prepared inactivated rotavirus (RV) as described previously (Figure S4A) (Burns et al., 1995; Kim et al., 2008). Groups of BALB/c mice challenged with RV (WT-RV) for 2 weeks were asymptomatic and did not show any colon pathology (data not shown). Of note, more attenuated colitis symptoms were observed in RV-treated mice (WT-DSS+RV) than in non-treated (WT-DSS) mice (Figure S4). Unlike RV-untreated mice, no significant weight loss or clinical symptoms were observed in RV-treated mice after DSS administration (Figure S4B). Milder DSS-induced colitis in RV-treated mice was confirmed by colon length and histopathologic analysis of the colon tissues (Figures S4C and S4D). RV treatment also significantly reduced the numbers of infiltrated $CD11b^{+}Gr\text{-}1^{hi}$ neutrophils and $CD11b^{+}F4/80^{+}$ macrophages (Figure S4E). To further determine the protective role of RV on intestinal inflammation, we assessed the secretion of cytokines and chemokines in colon tissue homogenates. As expected, there were significantly lower amounts of cytokines (e.g., IL-6 and IFN-γ) and chemokines (e.g., KC) in the colon tissues of RV-treated mice (Figure S4F). Overall, we found that reconstitution of an enteric virus such as non-replicable RV had a beneficial effect for DSS-induced colitis via TLR3+7 signaling.

TLR3+7 Signaling by Recognition of Enteric Viruses Upregulates Innate Immune Defense Molecules during Colitis

To investigate how TLR3+7 signaling, by recognition of enteric viruses, affects intestinal inflammation, we compared gene-expression profiles in the colon tissues of PBS-treated (DSS), AV cocktail-treated (DSS-AV), and TLR3+7 agonist-treated (DSS-Ta) WT mice after exposure to DSS. Some 300 genes were higher or lower (i.e., changed $\geq$ 2-fold) in DSS-AV and DSS-Ta mice compared with the DSS group (Figure S5). By gene ontology analysis, we selected 55 differentially expressed genes (DEGs) that were shared between DSS-AV and DSS-Ta mice (Figure S5). These DEGs fell into two categories by expression in DSS-AV and DSS-Ta mice: 27 were upregulated in DSS-AV mice but downregulated in the DSS-Ta group, consistent with the intestinal pathology of DSS-AV or DSS-Ta mice. By pathway analysis *S100a8*, *S100a9*, *Saa3*, *Ccl4*, and *Il1b* were the central genes in the axis of NF-κB and inflammation, assuming that TLR3+7 signaling can regulate intestinal inflammation by affecting the NF-κB pathway (Figure 4A and Table S2). Although 55 genes were differentially expressed in the DSS-AV and DSS-Ta groups, it was not easy to distinguish regulatory from phenotypically expressed genes. To exclude the pathologically expressed genes, we tried to select the DEGs only in AV- or Ta-treated groups (Figure 4B and Table S3). Most of these genes were related to nucleotide-binding activity, ion transport, and ion-dependent signaling molecules. As expected, we found upregulated molecules of innate immune defenses (e.g., *Irf7* and *Dhx58*) in DSS-Ta mice (Figure 4B and Table S3). We selected eight genes from microarray data and then ran real-time PCR to confirm the results. All gene expression were confirmed (Figure 4C). To search the regulatory genes for an association with intestinal inflammation, we used physical interaction analysis (GeneMANIA) (Montojo et al., 2010) to focus on genes that could influence the inflammatory (e.g., NF-κB) pathway. Of note, *Adra2a* and *Npy* were displayed as regulatory genes and were linked to the NF-κB pathway through cyclic AMP (cAMP)-dependent binding molecules (CREB) (Figure 4D). We next focused on NF-κB activity because CREB protein competes with NF-κB for a required cofactor CREB-binding protein, thereby limiting NF-κB activity (Parry and Mackman, 1997). NF-κB activity was increased in the colon tissues of AV-treated mice but reduced in the TLR3/7 Ta-treated mice (Figure 4E). The modulated NF-κB activity by enteric virus load in the colon was confirmed by immunostaining with anti-NF-κB p50 antibody (Figure 4F). Therefore, it was necessary to verify that TLR3+7 signaling can control intestinal inflammation by regulating the NF-κB-dependent pathway.

Recognition of Resident Enteric Virus through Both the TLR3 and TLR7 Pathways Is Required for Protection against Intestinal Inflammation

To further confirm our hypothesis that gut symbiosis might be maintained by recognition of gut-resident viral products by TLR3+7 signaling, we generated TLR3 and TLR7 double-deficient ($Tlr3^{-/-}Tlr7^{-/-}$) mice. Naive $Tlr3^{-/-}Tlr7^{-/-}$ mice appeared healthy at birth and showed normal growth in a pathogen-free environment but were more susceptible to DSS-induced colitis and had more severe weight loss and clinical symptoms than the TLR3 and TLR7 intact WT mice (Figure 5A). In addition, $Tlr3^{-/-}Tlr7^{-/-}$ mice started to die 7 days after DSS treatment, whereas all WT mice survived (Figure S6A). The colons of $Tlr3^{-/-}Tlr7^{-/-}$mice were significantly shorter than those of WT mice after DSS treatment (Figure 5B). Significant pathology in colons of $Tlr3^{-/-}Tlr7^{-/-}$ mice included damaged epithelial tissue, crypt distortion, and infiltration of inflammatory cells; WT mice had milder symptoms (Figure 5C). Histologic changes associated with severe colitis in $Tlr3^{-/-}Tlr7^{-/-}$ mice were confirmed by pathological scoring (Figure 5C). As expected, we found increased infiltration of $CD11b^{+}Gr\text{-}1^{hi}$ neutrophils and $CD11b^{+}F4/80^{+}$ macrophages in the colon tissues of $Tlr3^{-/-}Tlr7^{-/-}$ mice beginning 4 days after DSS treatment (data not shown). These findings were sustained until day 10 after DSS treatment (Figure 5D), consistent with the pathologic score. Neither PBS-treated WT nor $Tlr3^{-/-}Tlr7^{-/-}$ mice had significant differences in those cell subsets (data not shown). In order to further assess pathologic changes in the $Tlr3^{-/-}Tlr7^{-/-}$ mice, we analyzed the secreted amounts of cytokines and chemokines from colon tissue homogenates. Amounts of inflammatory cytokines (IL-6, IFN-γ, and TNF-α) and chemokines (KC, MCP-1, MIP-1α, and RANTES) were much higher in the colon tissues of $Tlr3^{-/-}Tlr7^{-/-}$ mice than in those of WT mice (Figure 5E). To determine whether TLR3 and TLR7 have redundancy in protection against intestinal inflammation, we gave *Tlr3* or *Tlr7* single-deficient mice DSS for 7 days and monitored them. Body weight changes, clinical symptoms, and colon lengths in *Tlr3* and *Tlr7* single-deficient mice were similar to those of WT mice, whereas $Tlr3^{-/-}Tlr7^{-/-}$ mice had severe colitis (Figure S6). These findings suggest that TLR3 and TLR7 signaling pathways play a protective role in intestinal inflammation.

Combined Effects of *TLR3* and *TLR7* Genetic Variations on Severity of Human IBD

In order to address the role of enteric virus signaling at onset and disease severity of IBD in humans, we investigated the

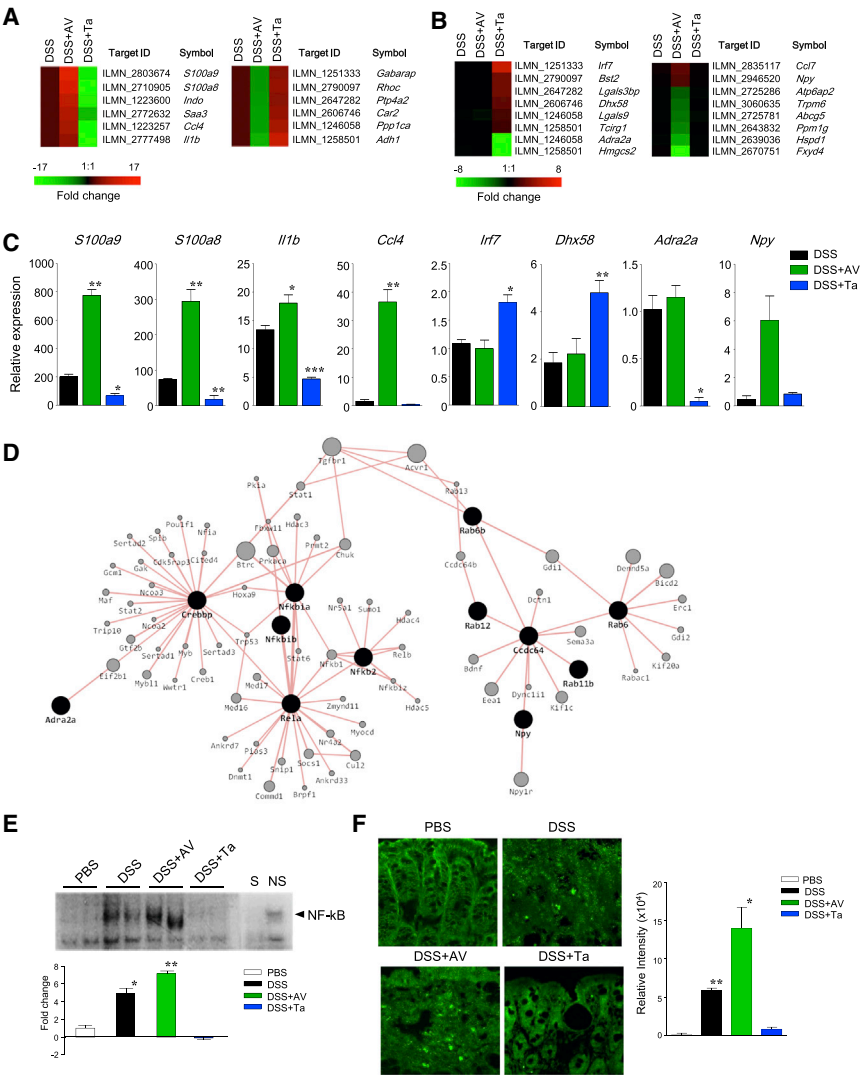

Figure 4. Genes for Intestinal Inflammation Are Regulated by TLR3+7 Signaling

(A) Subsets of differentially expressed genes (DEGs) (fold change > 2.0) shown on heat map. Representative 12 DEGs were significantly changed in a TLR3+7 signaling-dependent manner (shown as log_2-transformed fold-changes).

(B) Some genes were regulated only in AV- or Ta-treated conditions (fold change > 2.0): Representatives of 16 genes were changed only in AV- or in Ta-treated mice but were unchanged in DSS-treated mice.

(C) DEG expression levels were confirmed by real-time PCR. *$p < 0.05$, **$p < 0.01$ versus DSS group.

(D) Protein-protein interaction network generated with selected genes (e.g., *Adra2a*, *Npy*, *NFkB2*, *Rab6b*) as shown by GeneMANIA package (version 3.3) plugged into Cytoscape (version 3.0.1). Black and gray circles represent query and neighbor genes (i.e., genes known to interact), respectively. Large and small circles indicate statistical significances of interaction for each node as estimated by GeneMANIA with largest circles indicating greatest significance. Query proteins are always given the maximum node size; node size for related genes is inversely proportional to the rank of the gene in a list sorted by the gene score assessed by GeneMANIA.

(E) Specific NF-κB binding activity was determined by NF-κB probe. Specificity was confirmed by competitive reaction with overdose of non-radiolabeled NF-κB probe (S) or equivalent dose of non-radiolabeled CRE-1 probe (NS). The activity was quantificated using ImageJ software.

(F) Immunohistochemistry for p50-NF-κB in colon tissues. Swiss-rolled colon tissues were fixed with 4% para-formaldehyde and embedded in paraffin. Paraffin-embedded tissue sections were stained with p50-NF-κB antibody and further assessed by confocal microscopy. Relative intensity was analyzed by ImageJ software. *$p < 0.05$, **$p < 0.01$ versus PBS group.

associations of human *TLR3* and *TLR7* variants and susceptibility to IBD using direct sequencing and subsequent genotyping of the two gene variants. The study population consisted of 570 ethnically homogeneous Koreans including 174 with CD, 107 with UC, and 289 unrelated healthy controls. In the allelic association analysis, SNP rs 3775291 in *TLR3* was significantly associated with susceptibility to both UC and CD (Figure 6A). However, there was no significant difference in the allelic frequency of SNP rs3853839 in *TLR7* between patients with IBD and controls.

To evaluate the effects of *TLR3* and/or *TLR7* genetic variations (rs 3775291 and rs3853839) on the phenotypes of IBD, we compared the allele and genotype frequencies between patients with and without specific phenotypes. We found that patients with the two combined genetic variants had a higher cumulative rate of hospitalization than those with a single variant or without ($p = 0.005$; Figure 6B). When we analyzed the effects of each single *TLR3* or *TLR7* variant on the other disease outcomes including cumulative corticosteroid use, hospitalization, and surgery rates, we found that their effects were marginal to modest and negligible, respectively (Figure S7). Overall, these results strongly suggest that the TLR3+7-mediated host defense mechanism plays an indispensable role in the regulation of gut inflammation.

Colon pDCs Produce IFN-β in a TLR3- and TLR7-Dependent Manner during Inflammation

To clarify the TLR3+7-dependent protective immunity during gut inflammation, we first isolated monocytes (Mo; $CD11b^+Ly6G^-Ly6C^+$), conventional dendritic cells (cCDs; $MHCII^+CD11b^+CD11C^+$), and plasmacytoid dendritic cells (pDCs; $MHCII^+CD11b^-CD11C^+PDCA\text{-}1^+$) from colon of WT and $Tlr3^{-/-}Tlr7^{-/-}$ mice with DSS-induced colitis. Those isolated cells were stimulated with LPS or Poly I:C and IMQ for 24 hr in vitro, and then pro-inflammatory and anti-inflammatory cytokines were measured in the culture supernatant. As shown in Figure 7A, LPS stimulation elicited high levels of pro-inflammatory cytokines (IL-6 and TNF-α) by Mo and cDCs but not by pDCs from inflamed colon of WT mice. pDCs did not produce IL-6 and TNF-α in the presence of LPS or Poly I:C and IMQ. Most importantly, pDCs but not Mo and cDCs from inflamed colon of WT mice produced

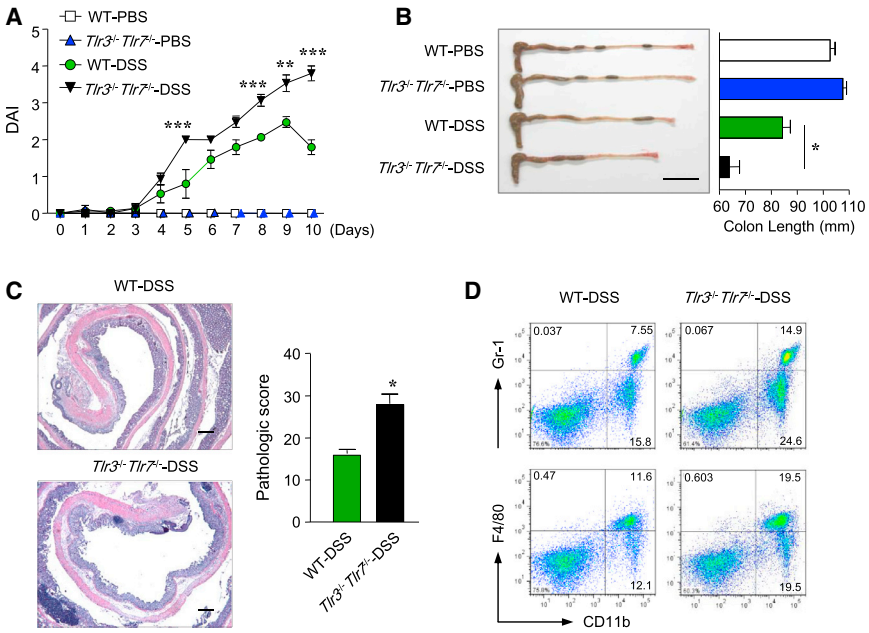

Figure 5. *Tlr3*$^{-/-}$*Tlr7*$^{-/-}$ Mice Are More Susceptible to DSS-Induced Colitis

BALB/c background WT and *Tlr3*$^{-/-}$*Tlr7*$^{-/-}$ mice were given 2.5% DSS in drinking water for 10 days.

(A) Disease activity index (DAI) was scored as described in Experimental Procedures.

(B) Colon length was measured 10 days after DSS treatment.

(C) Histologic changes and histopathologic scores were analyzed in a blinded manner. Results shown are representative of four independent experiments, each with ≥ 5 mice per group. Scale bar represents 100 μm.

(D) Infiltration of neutrophils (CD11b^{+}Gr-1^{hi}) and macrophages (CD11b^{+}F4/80^{+}) were analyzed in colon tissues of WT and *Tlr3*$^{-/-}$*Tlr7*$^{-/-}$ mice after DSS treatment by FACS analysis.

(E) Tissue homogenates from WT and *Tlr3*$^{-/-}$*Tlr7*$^{-/-}$ mice were prepared as described in Experimental Procedures. Cytokine and chemokine levels in colon tissues were measured by ProcartaPlex Multiplex Immunoassays. *p < 0.05, **p < 0.001, ***p < 0.001 versus WT-DSS group.

significantly higher levels of IFN-β when stimulated with Poly I:C and IMQ while LPS stimulation failed to do so (Figure 7B). No detectable levels of IFN-β were found in cell subsets from *Tlr3*$^{-/-}$*Tlr7*$^{-/-}$ mice (Figure 7B). In all experimental sets, IFN-α levels were below detectable limits (data not shown). Taken together, these results suggest that resident intestinal viruses through TLR3- and TLR7-mediated IFN-β secretion by pDCs play a protective role in gut inflammation.

DISCUSSION

We show here that mice pretreated with an AV cocktail had more severe colitis than those that were not treated. Treatment with TLR3+7 agonists and inactivated RV ameliorated colitis symptoms and *Tlr3*$^{-/-}$*Tlr7*$^{-/-}$ mice were susceptible to DSS-induced colitis. In our study of humans with IBD, those with combined *TLR3+7* genetic variants have higher cumulative hospitalization rates. We also found that TLR3+7 agonists stimulated IFN-β secretion by pDCs during inflammation. We propose that resident intestinal viruses ameliorate inflammation through secretion of anti-inflammatory cytokines such as IFN-β in a TLR3+7-dependent manner.

Gut homeostasis is tightly controlled by intricate cross-talk among genetic factors, the host immune system, and environmental factors such as microbiota. Breakdown of balanced interaction of homeostatic factors results in gut inflammation. Although microbial imbalance is crucial for the pathogenesis of intestinal inflammation, prior studies have focused solely on commensal bacteria. However, metagenomic analysis shows that gut microbiota consist not only of bacteria but also of fungi and viruses (Phan et al., 2011; Reyes et al., 2010). A previous epidemiologic study showed that resident viruses can be pathogens but some viruses can inhabit the body without pathogenic changes (Duerkop and Hooper, 2013). Resident viruses are found in humans in the oral cavity, nasopharynx, skin, and gastrointestinal and respiratory tracts (Bogaert et al., 2011; Foulongne et al., 2012; Lazarevic et al., 2012). The gastrointestinal tract is populated mainly with bacteriophages and eukaryotic viruses such as adenoviruses, herpesviruses, and uncharacterized eukaryotic viruses (Kim et al., 2011; Reyes et al., 2010). Moreover, RNA viruses are routinely detected in asymptomatic infants and individuals recovering from acute gastroenteritis (Grohmann et al., 1991; Matson et al., 1990). There have been questions as to how resident viruses in the gut can lack pathogenicity and how the resident virus-host immune system is altered in disease.

In this study, we found that AV treatment resulted in fewer viral particles and community-wide alterations in resident gut viral DNA and RNA metagenomes and led to more severe colitis. On the other hand, activation of innate immune signals by RV ameliorates gut inflammation. Thus, gut-resident viruses could have either adverse or beneficial immunomodulatory effects

A

gene	rs number	genotype	CD	p-value	OR	UC	p-value	OR	control
			(n=174)			(n=107)			(n=289)
TLR3	rs3775291 Dominant	TC/TT	84 (48.3%)	0.0009	1.906 (1.296 -2.803)	55 (51.4%)	0.0007	2.160 (1.375 -3.393)	95 (32.9%)
		CC	90 (51.7%)			52 (48.6%)			194 (67.1%)
			(n=172)			(n=107)			(n=93)
TLR7	rs3853839 Recessive	CC	33 (19.2%)	0.068	0.580 (0.323-1.044)	23 (21.5%)	0.22	0.669 (0.352 -1.273)	27 (29.0%)
		GG/CG	139 (80.8%)			84 (78.5%)			66 (71.0%)

CD, Crohn's diseases; UC, ulcerative colitis; OR, odds ratio.

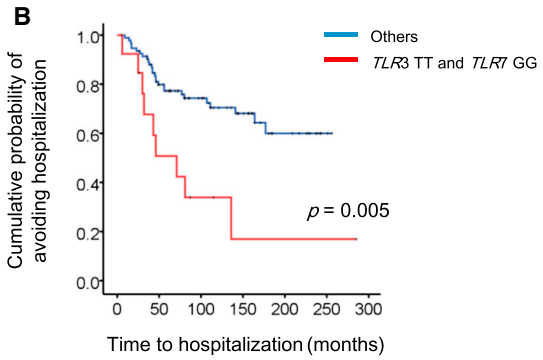

Figure 6. Combined Effects of *TLR3* and *TLR7* Genetic Variations on Severity of IBD in Humans

(A) The associations of human *TLR3* and *TLR7* variants and susceptibility to IBD using direct sequencing and subsequent genotyping of the two gene variants.

(B) Combined effects of *TLR3* and *TLR7* genetic variations on severity of ulcerative colitis in humans. Cumulative hospitalization-free survival after remission was calculated by Kaplan-Meier method, with differences determined by log-rank test.

and account for greater susceptibility to DSS-induced gut inflammation. Previous studies found enriched viral particles and genotypic differences of gut bacteriophages in patients with CD (Lepage et al., 2008; Pérez-Brocal et al., 2013; Wagner et al., 2013). In addition, chronic viral infections by herpesviruses or endogenous retroviruses are linked to origin of or exacerbation of IBD (Antony et al., 2004; Kandiel and Lashner, 2006; Schunter et al., 2007). A recent comparative cohort study of patients with CD and UC suggested that an increase in *Caudovirales* bacteriophage richness was significantly correlated with the disease pathogenesis (Norman et al., 2015). Our results are consistent with IBD-specific viral alterations without a reduction in bacterial diversity and richness, indicating that an expansion of bacteriophages is involved in severe DSS-induced colitis independent of bacterial dysbiosis. On the other hand, a recent study showed that MNV was beneficial to the host by inducing gut epithelial and lymphoid cell differentiation and that it played a protective role against bacterial pathogens (Kernbauer et al., 2014). In our study, however, MNV was not detected in the feces of naive BALB/c mice before or after AV treatment (data not shown). As part of the extended metagenome in normal individuals, it is of note that gut-resident viruses contribute to maintaining gut homeostasis by eliciting anti-inflammatory innate immune responses and that suppression of resident viruses and alteration of community-wide are deeply involved in the pathogenesis of gut inflammation.

AV cocktail treatment influences the community composition of gut microbiota and resident viruses, although no underlying mechanism has been elucidated. The majority of resident viruses are bacteria-infecting viruses (bacteriophages) and their genetic stability and functional gene modules are characterized as being lysogenic (Reyes et al., 2010), indicating that gut phage activity is largely dependent on the bacterial host system. Suppression of AV agents on viral activity might be mediated by disrupting viral transcription and replication processes (Crotty et al., 2002), which likely affect phage replication and transcription, particularly by acyclovir. It is also possible that suppression of resident gut viral activity alters host mucosal immune reactions, which subsequently change the community composition of the gut microbiota. In our study, we show that the alteration of resident gut viral activity by AV cocktail treatment is associated with changes in particular bacterial taxa. The bacterial flagellin induces pro-inflammatory responses from gut epithelial cells and the recognition of those flagellated bacteria correlates with colitis severity in murine colitis models and in patients with IBD (Vijay-Kumar et al., 2010). Of note, many of the flagellated gut bacteria were assigned to the *Lachnospiraceae* family (Berry et al., 2012; Nakanishi et al., 2015), as also shown in our study. This underscores the observation that AV agents influence the community composition of the gut microbiota in part and might contribute to increased severity of gut inflammation in AV-treated mice with DSS-induced colitis.

The inflammatory symptoms observed in WT mice activated by innate signals with TLR agonists was confirmed in *Tlr3*$^{-/-}$ *Tlr7*$^{-/-}$ mice with DSS-induced colitis, indicating that enteric viruses are potentially linked to the pathogenesis of intestinal inflammation-mediated TLR innate signaling. Viral products from resident viruses might be recognized by either TLRs, RIG-I-like receptors (RLRs), or nucleotide oligomerization domain-like receptors (NLRs) (Kanneganti et al., 2006; Takeuchi and Akira, 2010). RLRs are cytoplasmic proteins consisting of, RIG-I, MDA5, and LGP2, which sense dsRNA or RNA with 5′-triphosphate ends (Yoneyama et al., 2004), whereas Nalp3, an NLR, detects the presence of dsRNA (Kanneganti et al., 2006). Interestingly, RIG-I-deficient mice spontaneously developed a colitis-like phenotype with increased susceptibility to DSS-induced colitis (Wang et al., 2007). Similarly, mitochondrial antiviral signaling protein (MAVS)-deficient mice developed severe mortality and morbidity in the DSS-induced colitis model (Li et al., 2011). Nalp3-deficient mice were normal at steady

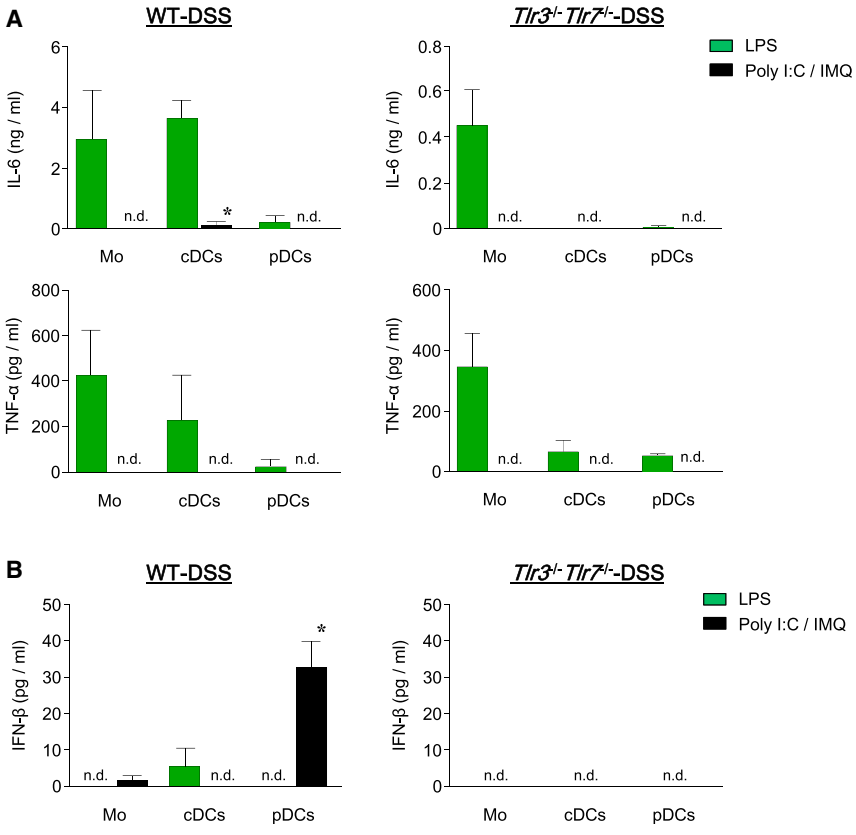

Figure 7. IFN-β Production in pDCs Was Enhanced during Gut Inflammation through TLR3 and TLR7 Signals

Mononuclear cells were isolated from colon tissues of WT (n = 5) and *Tlr3*$^{-/-}$*Tlr7*$^{-/-}$ mice (n = 5) after 2.5% DSS treatment. Three major populations such as monocytes (Mo; CD11b^{+}Ly6G^{-}Ly6C^{+}), conventional dendritic cells (cDCs; MHCII^{+}CD11b^{+}CD11C^{+}), and plasmacytoid DCs (pDCs; MHCII^{+}CD11b^{-}CD11C^{+}PDCA1^{+}) were sorted by FACSAria sorter and stimulated for 24 hr with LPS (1 μg/ml) or Poly [I:C] (5 μg/ml) and Imiquimod (5 μg/ml). TNF-α and IL-6 (A) and IFN-β (B) levels in culture supernatants were measured by ProcartaPlex Multiplex Immunoassays. Each value was normalized with that of the "cell only" group (no stimulation). Results shown are representative of three independent experiments. *p < 0.05 versus LPS-stimulated group; n.d., not detected.

state, but exhibited severe colitis after DSS treatment (Zaki et al., 2010). Although further studies are required to determine which innate signal is a main pathway for enteric viruses associated immune responses, our findings suggest that resident viruses play a protective role in gut homeostasis.

In order to determine the clinical relevance of our in vitro and in vivo data, we investigated the associations of human *TLR3* and *TLR7* variants and susceptibility to IBD using direct sequencing and subsequent genotyping of the two gene variants. IBD, a chronic intestinal inflammatory condition of unknown causes, includes patients with CD and UC. Although its precise pathogenesis is unknown, IBD is believed to result from interactions of genetic, microbial, and immunological factors that induce intestinal inflammation (Xavier and Podolsky, 2007). Our analysis of *TLR3* and *TLR7* in humans was consistent with our findings in a murine model. The combined mutations of the two genes significantly affected patient outcome in the UC group. In support of our results, others reported that *TLR3* was significantly downregulated in epithelial cells of patients with active IBD (Cario and Podolsky, 2000). Although *TLR3* or *TLR7* genetic variants were not identified in a genome-wide association study (GWAS) as IBD susceptibility genes, they might affect disease severity. Moreover, a single gene mutation among the two genes did not affect disease development, similar to our observation that single *Tlr3*$^{-/-}$ or *Tlr7*$^{-/-}$ mice did not develop more severe DSS colitis than WT mice.

Type I IFN signaling, which can be activated by TLR3+7 signaling cascades, is a possible mechanism for the protective effects of enteric viruses on intestinal inflammation. Others have reported that type I IFN induced by TLR9, TLR3, or TLR7 agonists prevents experimental colitis (Katakura et al., 2005; Sainathan et al., 2012; Vijay-Kumar et al., 2007). A previous study showed *Ifnar1*$^{-/-}$ mice were hypersensitive to DSS-induced colitis and administration of recombinant IFN-β produced anti-inflammatory effects (Katakura et al., 2005). Moreover, a recent study showed that beneficial effects of murine norovirus infection are dependent on type I IFN responses (Kernbauer et al., 2014). In our study, pDCs from inflamed colon produced predominant levels of IFN-β by stimulation of TLR3+7 agonists (i.e., Poly I:C / IMQ) while Mo and cDCs mainly produced IL-6 and TNF-α by stimulation of TLR4 agonist (i.e., LPS). Our results clearly indicate that resident virus elicits protective immunity through TLR3+7-mediated IFN-β by pDCs in the inflamed gut.

In the past, intestinal viruses have been thought to be detrimental or neutral to the host; however, as a result of our findings we propose that viruses have a role as resident commensals that promote protective immunity under inflammation conditions. Thus, in some circumstances, intestinal viruses might benefit and be useful for the host.

EXPERIMENTAL PROCEDURES

Mice

BALB/c mice were purchased from Charles River Laboratories (OrientBio). *Tlr3*$^{-/-}$ mice (BALB/c background) and *Tlr7*$^{-/-}$ mice (BALB/c background), kindly provided by Professor Shizuo Akira (iFrec, Osaka University), were crossed to generate *Tlr3*$^{-/-}$*Tlr7*$^{-/-}$ mice. All mice were maintained under specific pathogen-free conditions in the experimental facility at the Asan Biomedical Research Center where they received sterilized food and water ad libitum. All animal experiments described were approved by Asan Biomedical Research Center Institutional Animal Care and Use Committee.

Induction of DSS Colitis

Mice received 2.5% (w/v) DSS (MP Biomedicals) ad libitum in drinking water for 7 or 9 days and then switched to regular drinking water. The amount of DSS intake per mouse was recorded. There were no differences in intake

between mouse strains. Mice were weighed every day to determine percentage weight changes. This was calculated as percent body weight change = (weight at day X / weight at day 0) × 100. Animals were monitored clinically for rectal bleeding, diarrhea, and general signs of morbidity, including hunched posture and failure to groom.

Enumeration of Fecal VLPs

Fecal VLPs were counted as previously described (Thurber et al., 2009). In brief, a 0.5 g fecal sample was suspended with 10 ml of 0.02 μm filtered sterilized saline magnesium buffer (SM buffer; 100 mM NaCl, 8 mM $MgSO_4$, 50 mM Tris-HCl [pH 7.4], and 0.002% gelatin). The suspension was centrifuged again at 2,500 × *g* for 10 min at 4°C and the supernatant was filtered with 0.45 μm and 0.22 μm pore size syringe filters (Millipore) to remove cellular cells. For detailed methodology, see the Supplemental Experimental Procedures.

Depletion of Gut Enteric Virus

Mice were provided ribavirin (30 mg/kg; Roche Life Sciences), lamivudine (10 mg/kg; GlaxoSmithKline), and acyclovir (20 mg/kg; GlaxoSmithKline) intragastrically daily for 10 days prior to beginning DSS treatment. The treatment strategy with AV cocktail was based on preclinical studies of the agents (Field and De Clercq, 1981; Morrey et al., 1999; Sidwell et al., 1972).

DNA Extraction and Sequencing

The procedures used for VLP-derived nucleic acid extraction were as described (Kim et al., 2011). Briefly, the 0.22 μm filtrate was adjusted to 1.12 g ml^{-1} CsCl density and loaded onto the top of the 1.7, 1.5, and 1.3 g ml^{-1} CsCl densities. Samples were centrifuged at 4°C at 60,000 × g for 2 hr, and a 1.5–1.3 g ml^{-1} fraction was collected for double-stranded and single-stranded DNA and RNA viruses (Thurber et al., 2009). The fraction was treated with 0.2 vol of chloroform for 10 min at room temperature, and centrifuged at 2,000 × g for 5 min. The aqueous phase was desalted and concentrated using centrifugal concentration filters (Amicon Ultra-15, 30 kDa, Millipore). The concentrate was treated with DNase I (2.5 U ml^{-1}; Ambion) for 1 hr at 37°C to remove cellular DNA. For DNA viruses, we used half of the concentrate to extract VLP-derived DNA metagenome using the QIAmp MinElute Viral Spin Kit (QIAGEN). For RNA viruses, the other half of the concentrate was used for VLP-derived RNA metagenome using the RNeasy Mini Kit (QIAGEN). First strand cDNA was synthesized from the extracted RNA using SuperScript™ III Reverse Transcriptase with random primers (Invitrogen), according to the manufacturer's instruction. The VLP-derived DNA genomes and cDNA-synthesized RNA genomes were amplified using the Illustra Genomiphi V2 DNA Amplification Kit (GE Healthcare), according to the manufacturer's instruction. The amplified DNA samples were sequenced using Illumina MiSeq sequencing (300 bp × 2) (Illumina).

Fecal VLP-Derived Metagenome Analysis

Raw paired-end reads were filtered out based on a minimum mean quality score of 30 and no uncalled bases using Preprocessing and Information of SEQuences (PRINSEQ, v.0.20.4). Exact duplicates and singletons were also filtered out. The paired-end reads homologous to mouse reference genomes (BLASTn, *E*-value < 10^{-5}) were subsequently excluded. Microbial contamination was evaluated by searching for the reads homologous to 16S rRNA gene sequence database (BLASTn, *E*-value < 10^{-5}) in the Ribosomal Database Project Release 9. For more informative gene prediction and annotation (Pride et al., 2012; Wommack et al., 2008), the paired-end reads for each DNA or RNA dataset were hybrid-assembled to contigs using de novo assembler IDBA-UD (v1.1.1). The contigs were clustered using CD-HIT-EST (v4.6.1) at minimal 90% identity and minimal 90% alignment. The sequence abundance of the contigs was calculated by counting the number of sequences falling into each contig using Bowtie2 alignment (v2.2.3). The abundance of the non-redundant contigs was determined by dividing the coverage per base pair by the length of the contig. Based on contig abundance, the number of sequences for each sample was rarefied (900,000 reads for DNA data; 690,000 reads for RNA data) to normalize different sequencing depths using QIIME (v1.9.0) (Caporaso et al., 2010). By using comparative matrices, the distance matrices were calculated based on Jaccard (presence/absence) and Hellinger (abundance) distances. The community comparisons were visualized by PCoA using the QIIME package. The contigs were compared against NCBI RefSeq viral genomes (last updated 6 Nov 2014) and non-redundant protein database (last updated 29 March 2015) using tBLASTx and BLASTx searches (*E*-value < 10^{-5}), respectively. The most significant BLAST hit was used for contig identification.

16S rRNA Gene-Based Bacterial Community Analysis

The procedures for bacterial community analysis of fecal samples before and after AV treatment (n = 5 each) were done as described previously (Kim et al., 2013). Metagenomic DNA extraction was performed using DNA Stool Mini Kit (QIAGEN) as described (Zoetendal et al., 2006). For detailed methodology, see the Supplemental Experimental Procedures.

Reconstitution with Inactivated RV or TLR Ligands

Murine EC type RV was prepared from intestinal homogenates of 5- to 6-day-old suckling BALB/c mice infected with RV (EC strain). The infectivity of the murine strains was determined in vivo in suckling mice and expressed as a diarrhea dose 50 (DD_{50}). Inactivated RV failed to replicate by abrogating expression of non-structural protein 3. Mice were given inactivated RV for 6 days prior to beginning and during DSS administration. To stimulate TLR3/7 directly, we challenged ligands for TLR3 (Poly [I:C], 10 mg/kg; Invitrogen) and TLR7 (Imiquimod, 10 mg/kg, Invitrogen) intraperitoneally during DSS treatment.

Microarray Analysis

Colon tissues were removed 8 days after DSS treatment (DSS) with antiviral cocktail (DSS+AV) or TLR 3+7 agonists (DSS+Ta) and washed with PBS. RNA from colon tissues was isolated with TRIzol (Invitrogen) reagent. cDNA microarray analysis was performed using a Mouse Ref-8 v2 Expression Bead Chip Kit (Illumina).

Human TLR3 and TLR7 Variants Study

Patients with IBD were recruited at the Yonsei University Medical Center, Severance Hospital. The diagnosis of CD or UC was determined based on clinical, endoscopic, radiologic, and histopathologic findings according to established guidelines (Lennard-Jones, 1989). Controls were defined as healthy individuals without symptoms or history of IBD or other chronic diseases. This study was approved by the Institutional Review Board of the Yonsei University College of Medicine and all participants provided written informed consent prior to entering the study. Demographic and clinical characteristics were obtained from the patients' medical records. Detailed methodology is in the Supplemental Experimental Procedures.

Statistical Analysis

GraphPad Prism software (GraphPad) was used for statistical analysis. Significant differences between two groups were analyzed with two-tailed paired t test or Mann-Whitney t test. Multiple groups were analyzed by two-way ANOVA followed by Bonferroni post hoc test (*$p < 0.05$; **$p < 0.01$; ***$p < 0.001$). All SNPs were tested for Hardy-Weinberg equilibrium in controls using Pearson's χ^2-test. When the Bonferroni correction was subsequently applied in order to correct the statistical bias due to multiple testing across two SNPs, the adjusted significance level was 0.05/2 = 0.025. The cumulative hospitalization-free survival after remission was compared using the Kaplan-Meier method, with differences determined by log-rank test. Multivariate regression analysis was performed using Cox's proportional hazards modeling.

ACCESSION NUMBERS

The EMBL-EBI accession number for VLPs-derived metagenomic sequences and the 16S rRNA gene sequences is PRJEB9505. All microarray data are available in NCBI's Gene Expression Omnibus public database under accession number GSE79241.

SUPPLEMENTAL INFORMATION

Supplemental Information includes seven figures, three tables, and Supplemental Experimental Procedures and can be found with this article online at http://dx.doi.org/10.1016/j.immuni.2016.03.009.

AUTHOR CONTRIBUTIONS

J.-Y.Y., M.-S.K., E.K., and J.H.C. designed and performed experiments, analyzed data, and wrote the manuscript; Y.-S.L., S.-U.S., S.-H.L., and Y.K. performed experiments; S.-H.S. and S.S.C. performed microarray data analysis; B.K. provided inactivated rotavirus; S.-Y.C. and H.-J.K. advised experiments; J.-W.B. and M.-N.K. conceptualized and supervised the study and wrote the manuscript.

ACKNOWLEDGMENTS

This work was supported by the Korean Healthcare Technology R&D Project, Ministry for Health, Welfare and Family Affairs, Republic of Korea HI12C06870000 (A120770 and A120176) and HI13C0016, and the National Research Foundation of Korea (NRF) funded by the Ministry of Science, ICT & Future Planning (MSIP) (2010-0029133, 2011-0028854, 2012-0000805, 2013R1A2A2A01067123, and 2015M3C9A2054299).

Received: November 5, 2015
Revised: December 14, 2015
Accepted: December 29, 2015
Published: April 12, 2016

REFERENCES

Antony, J.M., van Marle, G., Opii, W., Butterfield, D.A., Mallet, F., Yong, V.W., Wallace, J.L., Deacon, R.M., Warren, K., and Power, C. (2004). Human endogenous retrovirus glycoprotein-mediated induction of redox reactants causes oligodendrocyte death and demyelination. Nat. Neurosci. *7*, 1088–1095.

Basic, M., Keubler, L.M., Buettner, M., Achard, M., Breves, G., Schröder, B., Smoczek, A., Jörns, A., Wedekind, D., Zschemisch, N.H., et al. (2014). Norovirus triggered microbiota-driven mucosal inflammation in interleukin 10-deficient mice. Inflamm. Bowel Dis. *20*, 431–443.

Berry, D., Schwab, C., Milinovich, G., Reichert, J., Ben Mahfoudh, K., Decker, T., Engel, M., Hai, B., Hainzl, E., Heider, S., et al. (2012). Phylotype-level 16S rRNA analysis reveals new bacterial indicators of health state in acute murine colitis. ISME J. *6*, 2091–2106.

Bogaert, D., Keijser, B., Huse, S., Rossen, J., Veenhoven, R., van Gils, E., Bruin, J., Montijn, R., Bonten, M., and Sanders, E. (2011). Variability and diversity of nasopharyngeal microbiota in children: a metagenomic analysis. PLoS ONE *6*, e17035.

Burns, J.W., Krishnaney, A.A., Vo, P.T., Rouse, R.V., Anderson, L.J., and Greenberg, H.B. (1995). Analyses of homologous rotavirus infection in the mouse model. Virology *207*, 143–153.

Cadwell, K., Patel, K.K., Maloney, N.S., Liu, T.C., Ng, A.C., Storer, C.E., Head, R.D., Xavier, R., Stappenbeck, T.S., and Virgin, H.W. (2010). Virus-plus-susceptibility gene interaction determines Crohn's disease gene Atg16L1 phenotypes in intestine. Cell *141*, 1135–1145.

Caporaso, J.G., Kuczynski, J., Stombaugh, J., Bittinger, K., Bushman, F.D., Costello, E.K., Fierer, N., Peña, A.G., Goodrich, J.K., Gordon, J.I., et al. (2010). QIIME allows analysis of high-throughput community sequencing data. Nat. Methods *7*, 335–336.

Cario, E., and Podolsky, D.K. (2000). Differential alteration in intestinal epithelial cell expression of toll-like receptor 3 (TLR3) and TLR4 in inflammatory bowel disease. Infect. Immun. *68*, 7010–7017.

Crotty, S., Cameron, C., and Andino, R. (2002). Ribavirin's antiviral mechanism of action: lethal mutagenesis? J. Mol. Med. *80*, 86–95.

Duerkop, B.A., and Hooper, L.V. (2013). Resident viruses and their interactions with the immune system. Nat. Immunol. *14*, 654–659.

Field, H.J., and De Clercq, E. (1981). Effects of oral treatment with acyclovir and bromovinyldeoxyuridine on the establishment of maintenance of latent herpes simplex virus infection in mice. J. Gen. Virol. *56*, 259–265.

Finkbeiner, S.R., Allred, A.F., Tarr, P.I., Klein, E.J., Kirkwood, C.D., and Wang, D. (2008). Metagenomic analysis of human diarrhea: viral detection and discovery. PLoS Pathog. *4*, e1000011.

Foulongne, V., Sauvage, V., Hebert, C., Dereure, O., Cheval, J., Gouilh, M.A., Pariente, K., Segondy, M., Burguière, A., Manuguerra, J.C., et al. (2012). Human skin microbiota: high diversity of DNA viruses identified on the human skin by high throughput sequencing. PLoS ONE *7*, e38499.

Grohmann, G., Glass, R.I., Gold, J., James, M., Edwards, P., Borg, T., Stine, S.E., Goldsmith, C., and Monroe, S.S. (1991). Outbreak of human calicivirus gastroenteritis in a day-care center in Sydney, Australia. J. Clin. Microbiol. *29*, 544–550.

Hooper, L.V., Littman, D.R., and Macpherson, A.J. (2012). Interactions between the microbiota and the immune system. Science *336*, 1268–1273.

Kandiel, A., and Lashner, B. (2006). Cytomegalovirus colitis complicating inflammatory bowel disease. Am. J. Gastroenterol. *101*, 2857–2865.

Kanneganti, T.D., Body-Malapel, M., Amer, A., Park, J.H., Whitfield, J., Franchi, L., Taraporewala, Z.F., Miller, D., Patton, J.T., Inohara, N., and Núñez, G. (2006). Critical role for Cryopyrin/Nalp3 in activation of caspase-1 in response to viral infection and double-stranded RNA. J. Biol. Chem. *281*, 36560–36568.

Katakura, K., Lee, J., Rachmilewitz, D., Li, G., Eckmann, L., and Raz, E. (2005). Toll-like receptor 9-induced type I IFN protects mice from experimental colitis. J. Clin. Invest. *115*, 695–702.

Kernbauer, E., Ding, Y., and Cadwell, K. (2014). An enteric virus can replace the beneficial function of commensal bacteria. Nature *516*, 94–98.

Kim, B., Feng, N., Narváez, C.F., He, X.S., Eo, S.K., Lim, C.W., and Greenberg, H.B. (2008). The influence of $CD4^+$ $CD25^+$ $Foxp3^+$ regulatory T cells on the immune response to rotavirus infection. Vaccine *26*, 5601–5611.

Kim, M.S., Park, E.J., Roh, S.W., and Bae, J.W. (2011). Diversity and abundance of single-stranded DNA viruses in human feces. Appl. Environ. Microbiol. *77*, 8062–8070.

Kim, M.S., Hwang, S.S., Park, E.J., and Bae, J.W. (2013). Strict vegetarian diet improves the risk factors associated with metabolic diseases by modulating gut microbiota and reducing intestinal inflammation. Environ. Microbiol. Rep. *5*, 765–775.

Lazarevic, V., Whiteson, K., Gaïa, N., Gizard, Y., Hernandez, D., Farinelli, L., Osterås, M., François, P., and Schrenzel, J. (2012). Analysis of the salivary microbiome using culture-independent techniques. J. Clin. Bioinforma. *2*, 4.

Lennard-Jones, J.E. (1989). Classification of inflammatory bowel disease. Scand. J. Gastroenterol. Suppl. *170*, 2–6, discussion 16–19.

Lepage, P., Colombet, J., Marteau, P., Sime-Ngando, T., Doré, J., and Leclerc, M. (2008). Dysbiosis in inflammatory bowel disease: a role for bacteriophages? Gut *57*, 424–425.

Li, X.D., Chiu, Y.H., Ismail, A.S., Behrendt, C.L., Wight-Carter, M., Hooper, L.V., and Chen, Z.J. (2011). Mitochondrial antiviral signaling protein (MAVS) monitors commensal bacteria and induces an immune response that prevents experimental colitis. Proc. Natl. Acad. Sci. USA *108*, 17390–17395.

Matson, D.O., Estes, M.K., Tanaka, T., Bartlett, A.V., and Pickering, L.K. (1990). Asymptomatic human calicivirus infection in a day care center. Pediatr. Infect. Dis. J. *9*, 190–196.

Minot, S., Bryson, A., Chehoud, C., Wu, G.D., Lewis, J.D., and Bushman, F.D. (2013). Rapid evolution of the human gut virome. Proc. Natl. Acad. Sci. USA *110*, 12450–12455.

Montojo, J., Zuberi, K., Rodriguez, H., Kazi, F., Wright, G., Donaldson, S.L., Morris, Q., and Bader, G.D. (2010). GeneMANIA Cytoscape plugin: fast gene function predictions on the desktop. Bioinformatics *26*, 2927–2928.

Morrey, J.D., Bailey, K.W., Korba, B.E., and Sidwell, R.W. (1999). Utilization of transgenic mice replicating high levels of hepatitis B virus for antiviral evaluation of lamivudine. Antiviral Res. *42*, 97–108.

Nakanishi, Y., Sato, T., and Ohteki, T. (2015). Commensal Gram-positive bacteria initiates colitis by inducing monocyte/macrophage mobilization. Mucosal Immunol. *8*, 152–160.

Norman, J.M., Handley, S.A., Baldridge, M.T., Droit, L., Liu, C.Y., Keller, B.C., Kambal, A., Monaco, C.L., Zhao, G., Fleshner, P., et al. (2015). Disease-specific alterations in the enteric virome in inflammatory bowel disease. Cell *160*, 447–460.

Parry, G.C., and Mackman, N. (1997). Role of cyclic AMP response element-binding protein in cyclic AMP inhibition of NF-kappaB-mediated transcription. J. Immunol. *159*, 5450–5456.

Pérez-Brocal, V., García-López, R., Vázquez-Castellanos, J.F., Nos, P., Beltrán, B., Latorre, A., and Moya, A. (2013). Study of the viral and microbial communities associated with Crohn's disease: a metagenomic approach. Clin. Transl. Gastroenterol. *4*, e36.

Phan, T.G., Kapusinszky, B., Wang, C., Rose, R.K., Lipton, H.L., and Delwart, E.L. (2011). The fecal viral flora of wild rodents. PLoS Pathog. *7*, e1002218.

Pride, D.T., Salzman, J., Haynes, M., Rohwer, F., Davis-Long, C., White, R.A., 3rd, Loomer, P., Armitage, G.C., and Relman, D.A. (2012). Evidence of a robust resident bacteriophage population revealed through analysis of the human salivary virome. ISME J. *6*, 915–926.

Rakoff-Nahoum, S., Paglino, J., Eslami-Varzaneh, F., Edberg, S., and Medzhitov, R. (2004). Recognition of commensal microflora by toll-like receptors is required for intestinal homeostasis. Cell *118*, 229–241.

Reyes, A., Haynes, M., Hanson, N., Angly, F.E., Heath, A.C., Rohwer, F., and Gordon, J.I. (2010). Viruses in the faecal microbiota of monozygotic twins and their mothers. Nature *466*, 334–338.

Sainathan, S.K., Bishnupuri, K.S., Aden, K., Luo, Q., Houchen, C.W., Anant, S., and Dieckgraefe, B.K. (2012). Toll-like receptor-7 ligand Imiquimod induces type I interferon and antimicrobial peptides to ameliorate dextran sodium sulfate-induced acute colitis. Inflamm. Bowel Dis. *18*, 955–967.

Schunter, M.O., Walles, T., Fritz, P., Meyding-Lamadé, U., Thon, K.P., Fellermann, K., Stange, E.F., and Lamadé, W. (2007). Herpes simplex virus colitis complicating ulcerative colitis: A case report and brief review on superinfections. J. Crohn's Colitis *1*, 41–46.

Sidwell, R.W., Huffman, J.H., Khare, G.P., Allen, L.B., Witkowski, J.T., and Robins, R.K. (1972). Broad-spectrum antiviral activity of Virazole: 1-beta-D-ribofuranosyl-1,2,4-triazole-3-carboxamide. Science *177*, 705–706.

Takeuchi, O., and Akira, S. (2010). Pattern recognition receptors and inflammation. Cell *140*, 805–820.

Thurber, R.V., Haynes, M., Breitbart, M., Wegley, L., and Rohwer, F. (2009). Laboratory procedures to generate viral metagenomes. Nat. Protoc. *4*, 470–483.

Victoria, J.G., Kapoor, A., Li, L., Blinkova, O., Slikas, B., Wang, C., Naeem, A., Zaidi, S., and Delwart, E. (2009). Metagenomic analyses of viruses in stool samples from children with acute flaccid paralysis. J. Virol. *83*, 4642–4651.

Vijay-Kumar, M., Wu, H., Aitken, J., Kolachala, V.L., Neish, A.S., Sitaraman, S.V., and Gewirtz, A.T. (2007). Activation of toll-like receptor 3 protects against DSS-induced acute colitis. Inflamm. Bowel Dis. *13*, 856–864.

Vijay-Kumar, M., Aitken, J.D., Carvalho, F.A., Cullender, T.C., Mwangi, S., Srinivasan, S., Sitaraman, S.V., Knight, R., Ley, R.E., and Gewirtz, A.T. (2010). Metabolic syndrome and altered gut microbiota in mice lacking Toll-like receptor 5. Science *328*, 228–231.

Virgin, H.W. (2014). The virome in mammalian physiology and disease. Cell *157*, 142–150.

Wagner, J., Maksimovic, J., Farries, G., Sim, W.H., Bishop, R.F., Cameron, D.J., Catto-Smith, A.G., and Kirkwood, C.D. (2013). Bacteriophages in gut samples from pediatric Crohn's disease patients: metagenomic analysis using 454 pyrosequencing. Inflamm. Bowel Dis. *19*, 1598–1608.

Wang, Y., Zhang, H.X., Sun, Y.P., Liu, Z.X., Liu, X.S., Wang, L., Lu, S.Y., Kong, H., Liu, Q.L., Li, X.H., et al. (2007). Rig-I$^{-/-}$ mice develop colitis associated with downregulation of G alpha i2. Cell Res. *17*, 858–868.

Wommack, K.E., Bhavsar, J., and Ravel, J. (2008). Metagenomics: read length matters. Appl. Environ. Microbiol. *74*, 1453–1463.

Xavier, R.J., and Podolsky, D.K. (2007). Unravelling the pathogenesis of inflammatory bowel disease. Nature *448*, 427–434.

Yoneyama, M., Kikuchi, M., Natsukawa, T., Shinobu, N., Imaizumi, T., Miyagishi, M., Taira, K., Akira, S., and Fujita, T. (2004). The RNA helicase RIG-I has an essential function in double-stranded RNA-induced innate antiviral responses. Nat. Immunol. *5*, 730–737.

Zaki, M.H., Boyd, K.L., Vogel, P., Kastan, M.B., Lamkanfi, M., and Kanneganti, T.D. (2010). The NLRP3 inflammasome protects against loss of epithelial integrity and mortality during experimental colitis. Immunity *32*, 379–391.

Zhang, T., Breitbart, M., Lee, W.H., Run, J.Q., Wei, C.L., Soh, S.W., Hibberd, M.L., Liu, E.T., Rohwer, F., and Ruan, Y. (2006). RNA viral community in human feces: prevalence of plant pathogenic viruses. PLoS Biol. *4*, e3.

Zoetendal, E.G., Heilig, H.G., Klaassens, E.S., Booijink, C.C., Kleerebezem, M., Smidt, H., and de Vos, W.M. (2006). Isolation of DNA from bacterial samples of the human gastrointestinal tract. Nat. Protoc. *1*, 870–873.